Coupled Monte Carlo Simulation of Transient Electron-Phonon Transport in Nanoscale Devices

Yoshinari Kamakura*†, Nubuya Mori*†, and Kenji Taniguchi*
*Division of Electrical, Electronic and Information Engineering
Osaka University
2–1 Yamada-oka, Suita, Osaka 565–0871, Japan
†CREST, JST, Chiyoda, Tokyo 102-0075, Japan
Email: kamakura@si.eei.eng.osaka-u.ac.jp

Tomofumi Zushi and Takanobu Watanabe
Faculty of Science and Engineering
Waseda University
3–4–1 Ohkubo, Shinjuku-ku, Tokyo 169–8555, Japan

***Abstract*— Using a coupled Monte Carlo method for solving both electron and phonon Boltzmann transport equations, the transient electrothermal behaviors of nanoscale Si n-i-n device are simulated. The nonequilibrium optical phonon distribution is characterized by a temperature different from that of the acoustic phonons, and these two temperatures show different characteristics not only in the steady state, but also in transient conditions. It has been also suggested that the simulated transient response of the phonon temperatures can be practically described by the equivalent thermal circuit model, which is useful for, e.g., projecting the NBTI lifetime during the realistic circuit operations.**

I. Introduction

Growing heat dissipation is one of the main issues in today's IC chips limiting the reliability and performance. In the microscopic point of view, e.g., it has been pointed out that the nanoscale "hot spot" is generated in the MOSFET drain [1], [2], which may degrades the current drivability [3] and also worsen the negative bias temperature instability (NBTI) [4]. To explore this concern, ensemble Monte Carlo (MC) simulation coupled with phonon transport solver (solving simplified Boltzmann equation with relaxation time approximation) has been reported, and steady state simulations were demonstrated [5], [6].

In this study, we present a coupled MC simulation for both electron and phonon transport; the phonon MC simulation is more time consuming than the previous works, but various physical mechanisms can be implemented straightforwardly [7]. Using this new tool, we perform the electrothermal simulation of nanoscale Si devices especially focusing on the transient behavior, and then discuss the equivalent circuit model to describe the simulated results.

II. Simulation Method

We have simulated a simple 1-D n-i-n silicon device, inside which electrons and phonons were modeled as particles (Fig. 1). In the electron transport part, a standard MC model of [8] was employed for the electron-phonon scattering, etc, and the electron-electron scattering was also taken into account through the molecular dynamics approach [9], [10].

The spatial distribution of the heat generation rate $Q_p(x)$, where p denotes the phonon polarization, was monitored by

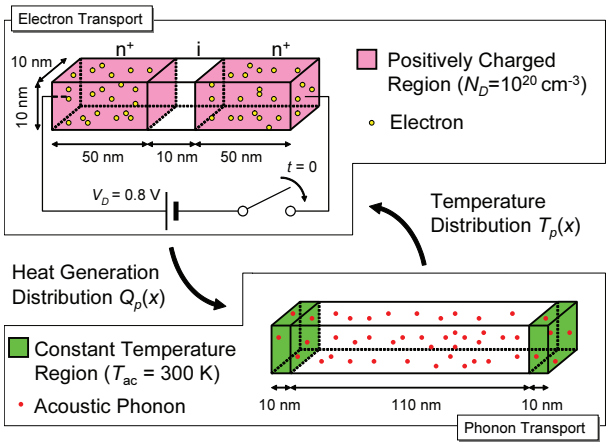

Fig. 1. Schematic view of the coupled MC Simulation for electron and phonon transport in 1-D n-i-n device with a channel length of 10 nm.

counting the net number of emitted phonons from the electrons [5]. In this study, the contribution of the optical phonons to the heat transport was assumed to be negligible, and their group velocity was approximated as zero, i.e., the optical phonon energy is constant ($\hbar\omega_{\rm op} = 61$ meV). Therefore, the thermal energy stored in the optical modes can only be dissipated through the conversion into the acoustic modes via phonon-phonon scattering, and we have treated this process by a relaxation time approximation [11] ($\tau_{\rm ph} = 10$ ps [1]). According to the heat power density transferred from the hot electrons and optical phonons, the acoustic phonons were generated and their random walks were simulated with a MC method. Although the poor heat conduction properties were pointed out in nanostructures [2], [12], we have assumed the bulk phonon characteristics in this study. For the simplicity, Debye approximation was adopted, and the constant acoustic phonon velocity ($v_{\rm ac} = 5.9$ km/s) was determined to reproduce the experimental specific heat of bulk Si [13], [14] (Fig. 2 (a)). The scattering mechanisms considered were phonon-phonon (having a role to help the phonons to follow an equilibrium distribution function), phonon-defect, and phonon-boundary interactions, for which all the parameters were taken from [15].

978-1-4244-7700-5/10/$26.00 ©2010 IEEE

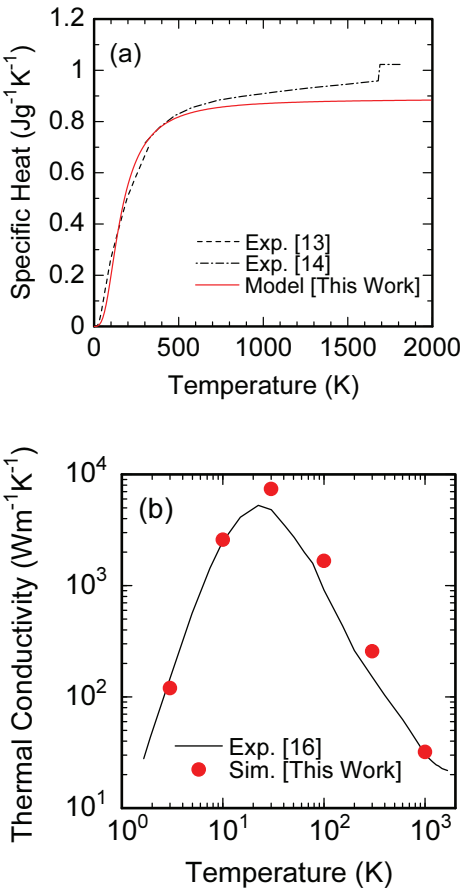

Fig. 2. Thermal properties of bulk Si calculated with the phonon MC simulator. (a) The specific heat and (b) the thermal conductivity are plotted as a function of temperature. The experimental data presented in [13], [14], [16] are also shown for comparison.

As shown in Fig. 2 (b), the simulated thermal conductivity exhibits good agreement with the experiment [16]. The local temperature distributions $T_p(x)$ were evaluated from the phonon distribution functions, and its information was used to update the electron-phonon scattering rate.

III. Simulation Results and Discussion

Fig. 3 shows the simulated heat distribution generated by the collision of electrons with lattice atoms. As is already reported, the power generation occurs almost within the drain in the quasi-ballistic transport regime [3], and its profile decays with a characteristic length of ~ 20 nm [5].

Fig. 4 shows the time evolution of $T_p(x)$; note that the growth of the acoustic phonon temperature $T_{\rm ac}$ is delayed than that for the optical phonon $T_{\rm op}$. This is because the hot electrons injected from the source mainly emit the optical phonons in the drain (see, Fig. 3), and a finite time is needed for optical phonons to decay into acoustic modes. We have also confirmed that such the localized heating in the drain, i.e., hot spot, slightly reduce the current density as shown in Fig. 5. The energy relaxation rate for the hot electrons is worsened due to the hot spot creation, which would degrade the ballisticity

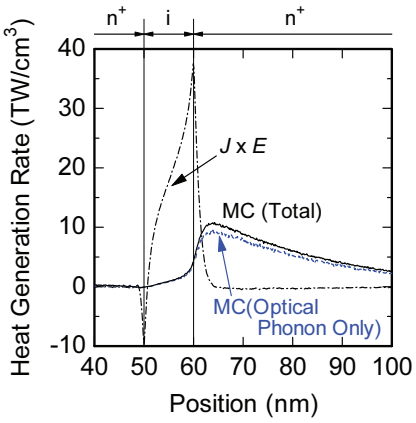

Fig. 3. The spatial distribution of heat generation rate $Q_p(x)$ simulated with the ensemble MC simulator for the electron transport. For comparison, the results estimated with the Joule heating formula ($J \times E$) are also plotted [3].

of the electron transport in 10 nm-scale Si channels [17]. Furthermore, we have also confirmed that the potential drop occurs in the source/drain region after the device is heated up, indicating the increased parasitic resistance. However, the raised temperature at the source edge enhances the electron injection from the source to the channel, which cancels out the current reduction caused by the effects discussed above.

In Fig. 6 (a), the local phonon temperatures at the drain edge are plotted as a function of time t after turning on the switch. In the initial stage, $T_{\rm op}$ increases as $\propto t$ and finally reaches the steady-state value, while the time delay (~ 10 ps $= \tau_{\rm ph}$) is occurred for heating the acoustic phonons. This behavior can be well described by the equivalent thermal circuit given in Fig. 6 (b), where an additional RC component is inserted into the conventional model used to consider the self-heating effect in the SPICE simulation [18]. In this model, the heat generation source at the drain with a power dissipation density

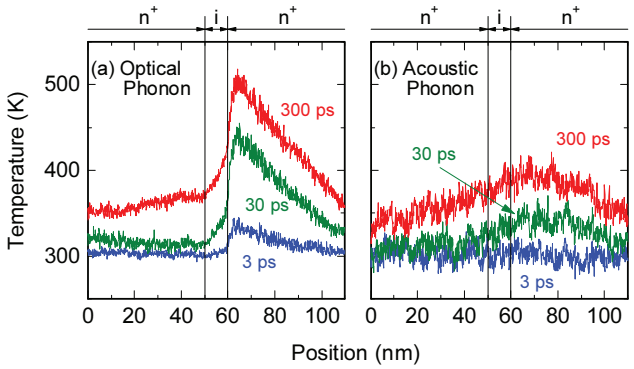

Fig. 4. Time evolution of the local temperature distributions $T_p(x)$ simulated with the ensemble MC simulator for the phonon transport. The temperatures of (a) optical phonons and (b) acoustic phonons are plotted as a parameter of time t after turning on the device.

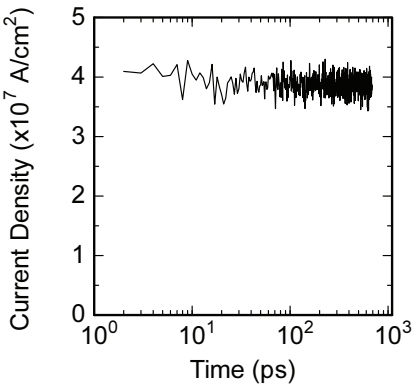

Fig. 5. The current density $J(t)$ observed during the coupled MC simulation. The data are plotted as a function of time t after turning on the device.

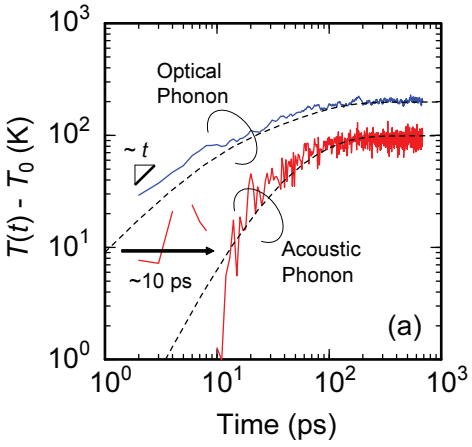

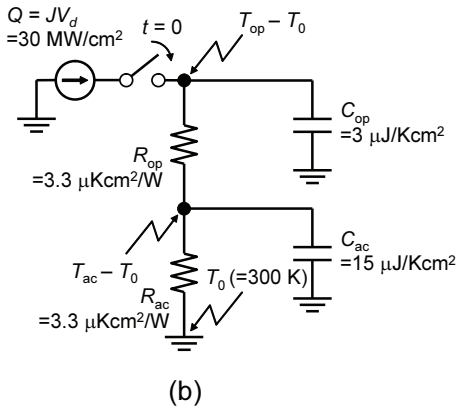

Fig. 6. (a) The local phonon temperatures at the drain edge (@$x = 63$ nm) are plotted as a function of time. Solid lines: the results simulated with the MC method. Dashed lines: the results calculated with the equivalent thermal circuit model given in (b), where the heat generation source ($Q = J \times V_d \sim 30$ MW/cm^2) is modeled as a constant current source, and the node voltages indicated by arrows correspond to the temperatures $T_{\rm op} - T_0$ and $T_{\rm ac} - T_0$, where T_0 (= 300 K) is the specified temperature at the both boundaries.

of $Q = J \times V_d \sim 30$ MW/cm^2 is modeled as a constant current source. The node voltages correspond to the temperatures $T_{\rm op} - T_0$ and $T_{\rm ac} - T_0$, where T_0 (= 300 K) is the specified temperature at the both boundaries of the simulated device (see, Fig. 1). Though the value of $C_{\rm op}$ is here determined by the fitting procedure, it can be related to the heat capacity of the hot spot, i.e., the specific heat (based on Einstein's model) multiplied by the hot spot size w:

$$C_{\rm op} = 3Nk_B \left(\frac{\hbar\omega_{\rm op}}{k_B T}\right)^2 \frac{e^{\hbar\omega_{\rm op}/k_B T}}{(e^{\hbar\omega_{\rm op}/k_B T} - 1)^2} \times w \ , \quad (1)$$

where N is the atom density. Substituting $T = 300$ K and $w = 23$ nm, (1) yields $C_{\rm op} = 3\ \mu$J/Kcm^2. Then the effective thermal resistance for optical phonons $R_{\rm op}$ is determined to make the RC time constant equal to $\tau_{\rm ph}$, i.e., $R_{\rm op} = \tau_{\rm ph}/C_{\rm op}$. This thermal circuit also well reproduces the simulation results for the pulse response (Fig. 7). Note that the hot spot is not instantaneously cooled down after turning off V_D, which is suggested to enhance the NBTI degradation in pMOSFETs just after the transition from the active to the standby states [4]. We believe that the proposed model is useful, e.g., to practically investigate the impact of the hot spot on the circuit reliability.

IV. Conclusion

Using the coupled MC technique for solving both electron and phonon Boltzmann transport equations, we have carried out the transient electrothermal simulation of nanoscale Si n-i-n device. We have also suggested that the simulated observations on the hot spot generation and dissipation can be practically described by the equivalent thermal circuit model, which is useful for projecting the NBTI lifetime during the realistic circuit operations.

Acknowledgment

This research was partially supported by the Ministry of Education, Culture, Sports, Science and Technology, Grant-in-Aid for Scientific Research on Particular Areas "Post Scale" (Grant No. 20035007).

References

[1] E. Pop, K. Banerjee, P. Sverdrup, R. Dutton, and K. Goodson, "Localized Heating Effects and Scaling of Sub-0.18 Micron CMOS Devices," in IEDM Tech. Dig., 2001, pp. 677–680.

[2] E. Pop, "Energy Dissipation and Transport in Nanoscale Devices," Nano Res., vol. 3, no. 3, pp. 147–169, March 2010.

[3] E. Pop, S.. Sinha, and K. E. Goodson, "Heat Generation and Transport in Nanometer-Scale Transistors," Proc. IEEE, vol. 94, no. 8, pp. 1587–1601, August 2006.

[4] Y. Wang, K. P. Cheung, A. Oates, and P. Mason, "Ballistic phonon enhanced NBTI," in Proc. IRPS, 2007, pp. 258–263.

[5] J. A. Rowlette and K. E. Goodson, "Fully Coupled Nonequilibrium Electron–Phonon Transport in Nanometer-Scale Silicon FETs," IEEE Trans. Electron Devices, vol. 55, no. 1, pp. 220–232, January 2008.

[6] K. Raleva, D. Vasileska, S. M. Goodnick, and M. Nedjalkov, "Modeling Thermal Effects in Nanodevices," IEEE Trans. Electron Devices, vol. 55, no. 6, pp. 1306–1316, June 2008.

[7] D. Lacroix, K. Joulain, and D. Lemonnier, "Monte Carlo transient phonon transport in silicon and germanium at nanoscales," Phys. Rev. B, vol. 72, no. 6, p. 064305, August 2005.

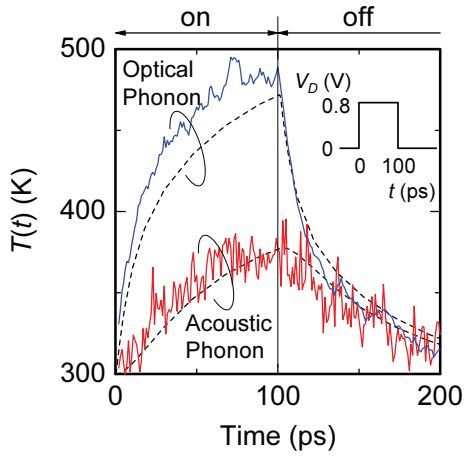

Fig. 7. Pulse response of local phonon temperatures at the drain edge. V_d was turned on at $t = 0$ and then turned off at $t = 100$ ps. Solid lines: the results simulated with the MC method. Dashed lines: the results calculated with the equivalent thermal circuit model given in Fig. 6 (b).

[8] C. Jacoboni and L. Reggiani, "The Monte Carlo method for the solution of charge transport in semiconductors with applications to covalent materials," Rev. Mod. Phys., vol. 55, no. 3, pp. 645–705, July 1983.

[9] R. P. Joshi and D. K. Ferry, "Effect of multi-ion screening on the electronic transport in doped semiconductors: A molecular-dynamics analysis," Phys. Rev. B, vol. 43, no. 12, pp. 9734–9739, April 1991.

[10] Y. Kamakura, H. Ryouke, and K. Taniguchi, "Ensemble Monte Carlo/Molecular Dynamics Simulation of Inversion Layer Mobility in Si MOSFETs–Effects of Substrate Impurity," IEICE Trans. Electron., vol. E86-C, no. 3, pp. 357–362, March 2003.

[11] A. Matulionis, J. Liberis, I. Matulionienė, M. Ramonas, L. F. Eastman, J. R. Shealy, V. Tilak, and A. Vertiatchikh, "Hot-phonon temperature and lifetime in a biased $Al_xGa_{1-x}N$/GaN channel estimated from noise analysis," Phys. Rev. B, vol. 68, no. 3, p. 035338, July 2003.

[12] T. Zushi, Y. Kamakura, K. Taniguchi, I. Ohdomari, and T. Watanabe, "Molecular Dynamics Simulation of Heat Transport in Silicon Nanostructures Covered with Oxide Films," Jpn. J. Appl. Phys., vol. 49, no. 4, p. 04DN08, April 2010.

[13] P. Flubacher, A. J. Leadbetter, and J. A. Morrison, "The heat capacity of pure silicon and germanium and properties of their vibrational frequency spectra," Philos. Mag., vol. 4, no. 39, pp. 273–294, March 1959.

[14] K. Yamaguchi and K. Itagaki, "MEASUREMENT OF HIGH TEMPERATURE HEAT CONTENT OF SILICON BY DROP CALORIMETRY," J. Therm. Anal. Cal., vol. 69, pp. 1059–1066, 2002.

[15] P. Chantrenne, J. L. Barrat, X. Blase, and J. D. Gale, "An analytical model for the thermal conductivity of silicon nanostructures," J. Appl. Phys., vol. 97, no. 10, p. 104318, May 2005.

[16] M. G. Holland, "Analysis of Lattice Thermal Conductivity," Phys. Rev., vol. 132, no. 6, pp. 2461–2471, December 1963.

[17] H. Tsuchiya and S. Takagi, "Influences of Elastic and Inelastic Scatterings on Ballistic Transport in MOSFETs," in Ext. Abst. Int. Conf. Solid State Devices and Materials, 2007, pp. 44–45.

[18] W. Jin, W. Liu, S. K. H. Fung, P. C. H. Chan, and C. Hu, "SOI Thermal Impedance Extraction Methodology and Its Significance for Circuit Simulation," IEEE Trans. Electron Devices, vol. 48, no. 4, pp. 730–736, April 2001.